



## Current topic

## Functional MRI of the placenta – From rodents to humans

R. Avni<sup>a</sup>, M. Neeman<sup>a, \*\*</sup>, J.R. Garbow<sup>b, \*</sup><sup>a</sup> Department of Biological Regulation, Weizmann Institute of Science, Rehovot 76100, Israel<sup>b</sup> Biomedical MR Laboratory, Mallinckrodt Institute of Radiology, Washington University, St. Louis, Missouri, United States

## ARTICLE INFO

Article history:  
Accepted 4 April 2015

Keywords:  
MRI  
Placenta  
Functional imaging  
Preclinical models

## ABSTRACT

The placenta performs a wide range of physiological functions; insufficiencies in these functions may result in a variety of severe prenatal and postnatal syndromes with long-term negative impacts on human adult health. Recent advances in magnetic resonance imaging (MRI) studies of placental function, in both animal models and humans, have contributed significantly to our understanding of placental structure, blood flow, oxygenation status, and metabolic profile, and have provided important insights into pregnancy complications.

© 2015 The Authors. Published by Elsevier Ltd. This is an open access article under the CC BY-NC-ND license (<http://creativecommons.org/licenses/by-nc-nd/4.0/>).

## 1. Introduction

Magnetic Resonance Imaging (MRI) is a versatile and powerful modality, which reveals, non-invasively, both structural and functional dynamic information, with high soft-tissue contrast and high spatial resolution. Functional MRI studies are particularly well-suited to the analysis of placental vascular physiology and function, as they provide a wide range of methods for detection of essential physiological parameters, such as blood flow, perfusion and oxygenation status. Many of these methods are based on the indicator dilution principle, in which a small amount of tracer introduced into the blood stream can be used for analysis of blood volume. However, in contrast to analytical determination of the tracer concentration in blood samples, in MRI, the tracer is detected indirectly by relying on a small number of fundamental contrast mechanisms, many of which will be described herein. In particular, this review will describe experiments that rely on changes in the major magnetic relaxation time constants,  $T_1$ ,  $T_2$  and  $T_2^*$ .  $T_1$  is the time constant for relaxation of the magnetic moment to its steady-state equilibrium condition along the main magnetic field of the MRI, and  $T_2/T_2^*$  are two time constants associated with the dispersion of the magnetization in the plane perpendicular to the magnetic field, and, thus, loss of a coherent signal from the radio frequency (rf) excited nuclei (These MRI terms and the different methodologies are explained more

fully in the [Supplementary Text](#)). Major challenges in modern day obstetrics include the identification of fetuses and mothers at high risk, diagnosis and quantification of placental insufficiency, and prediction of clinical outcome. In current clinical practice, screening and follow-up are largely based on ultrasound (US) assessments; however these measurements only provide an indirect estimate of placental function. Development of complementary, non-invasive MRI tools capable of assessing placental function may improve diagnosis of pregnancy complications, such as intrauterine growth restriction (IUGR) and preeclampsia (PE), and potentially assist in decisions on the timing of delivery and on perinatal outcome. Over the past few years, a number of MRI methods were developed and employed to study placental function in animal studies and in the clinical settings, including perfusion measurements using Dynamic Contrast Enhanced MRI (DCE-MRI), in which  $T_1$  is altered by intravenous administration of contrast agents [1–17]; perfusion measurements using arterial spin labeling (ASL), in which the measured  $T_1$  is affected by blood flow [18–23]; oxygenation studies using blood oxygen level dependent (BOLD), in which  $T_2^*$  changes reflect changes in hemoglobin saturation [24–31]; and oxygen enhanced (OE)  $T_1$  [31]. Diffusion weighted MRI (DW MRI) [32–42] probes the microstructural properties of tissue by measuring the incoherent motion of water within the tissue. Lastly, the dependence of resonance frequency on local chemical environment enables Magnetic Resonance Spectroscopy (MRS) as a tool for metabolic studies [43–46]. In this review, we will explain the basis of each of these methods and examine their application, starting from pre-clinical small-animal models, progressing to larger animal models and, finally, to human studies.

\* Corresponding author. Tel.: +1 314 362 9949; fax: +1 314 362 0526.

\*\* Corresponding author. Tel.: +972 8 9342487; fax: +972 8 9346264.

E-mail addresses: [michal.neeman@weizmann.ac.il](mailto:michal.neeman@weizmann.ac.il) (M. Neeman), [garbow@wustl.edu](mailto:garbow@wustl.edu) (J.R. Garbow).

## 2. Perfusion measurements using contrast agents

Dynamic contrast-enhanced MRI (DCE-MRI) is a widely used technique for *in vivo* mapping of vascular function, providing important insight into multiple parameters including blood flow, perfusion, fractional blood volume, extracellular volume fraction and vascular permeability. DCE-MRI experiments are based on the observed shortening of  $T_1$  following the administration of contrast agents, either low-molecular-weight or high-molecular-weight (macromolecular) chelates of Gd.

Placental perfusion and permeability were measured in pregnant mice at late gestation in both physiological and pathological settings. Placental perfusion was quantified using low-molecular-weight, Gd-chelate contrast agents, which, after intravenous administration to the mother, crossed the maternal-fetal barrier in the placenta. The acquired data were analyzed using a three-compartment, pharmacokinetic model [1,2]. This method has been implemented in detecting and investigating abnormal placental blood flow due to noradrenaline administration [3], and in rodent models of placental insufficiency [4,5]. Recently, the steepest slope model, a robust numerical method providing quantification of perfusion from a minimal set of DCE-MRI images, has been employed in a mouse model with the administration of GdDTPA, a clinical MRI contrast media. This model enabled separation of placental compartments, demonstrating high-flow and low-flow compartments in all placentas, and allowed quantification of mean perfusion values in each compartment separately (Fig. 1A) [6,7]. Placental perfusion has also been assessed using superparamagnetic iron oxide (SPIO) nanoparticles, and applied in a rat uterine artery ligation model of IUGR [8]. A significant advantage of this approach is that while Gd-based contrast agents are not recommended for use during human pregnancy, SPIOs are considered safe for clinical use. Thus, SPIO-based methods might become a tool for studying IUGR in humans.

The maternal circulation within the placenta has been previously investigated by us, at different developmental stages, using a macromolecular contrast agent, in which chelated Gd was covalently linked to albumin [9]. Since maternal albumin does not cross the fetal-maternal placenta barrier, the analysis of maternal circulation within the placenta is not confounded by transfer to the fetal circulation, as it can be with conventional Gd chelates. Using this methodology, it was possible to differentiate normal placentas from placentas undergoing resorption, and to resolve strain-specific differences [9]. Additionally, the effect of Akt1, a major mediator of angiogenesis, on placental vascular function was investigated [10].

DCE-MRI has been applied to assess perfusion in primate placenta, using manganese chloride [11], and standard Gd-based chelates [12,13]. Frias et al., was able to construct three-dimensional (3D) maps of placental structure, identifying placental vascular domains, consistent with placental histopathology. Furthermore, volumetric flow estimated in each perfusion domain closely matched the blood flow through the uterine artery, as measured by Doppler ultrasound [13].

The routine use of Gd chelates during human pregnancy is considered controversial, due to possible risks to fetal development. Conventional Gd agents have been administered intravenously during human pregnancy in rare cases involving women with a specific medical indication for DCE-MRI, typically the investigation of conditions that are considered potentially life threatening to the mother [14–16]. In a study undertaken a few hours prior to delivery by caesarean section, Brunelli, et al., used administration of gadoterate melamine to demonstrate that perfusion was homogeneous in normal placenta, whereas in pregnancies with severe IUGR, placental circulation was severely

compromised, displaying a slow intervillous blood flow, and many patchy non-perfused areas (Fig. 1B) [17].

These studies suggest that while DCE-MRI cannot be indicated for routine clinical prenatal follow-up of normal pregnancy, it is a robust method for measuring placental perfusion, and, thus, may offer valuable information for basic understanding of the etiology of placental diseases that may be translatable to humans.

## 3. Perfusion and flow measurements using endogenous MRI contrast

Translation of methods for measuring placental function from pre-clinical to clinical settings would be aided greatly by imaging protocols that do not require administration of an exogenous contrast agent. By magnetically tagging blood in the feeding artery (intrinsic contrast) and measuring its concentration in perfused tissue a short time later, Arterial Spin Labeling (ASL) methodology enables quantification of tissue perfusion. A time scale of seconds, characteristic of perfusion and nutrient exchange rates into the placenta, is accessible by ASL. With appropriate kinetic modeling, ASL allows quantitative assessment of important physiological vascular parameters, including perfusion, and blood flow.

Based on a modification of the ASL method, we reported a novel MRI tool, termed Bi-Directional ASL (BD-ASL), which enabled non-invasive determination of fetal order along the uterine horn in mice from the pattern of uterine versus ovarian maternal blood flow [18]. Together with fluorescence imaging methods, these experiments provided new insights into the structure and function of the complex architecture of the uterine maternal vasculature in multi-fetal pregnancies. Placental perfusion patterns suggest a collateral perfusion of the placenta, with separate arterial input from each of the feeding arteries, namely the uterine artery and uterine branch of ovarian artery (Fig. 2A). In addition, BD-ASL was utilized to understand the genetic and environmental factors that affect placental function, demonstrating the hemodynamic influence of individual fetuses on their nearest neighbors [19].

Flow-sensitive alternating inversion recovery (FAIR), a derivative of the ASL technique, has been implemented in several investigations of human placenta. In normal pregnancies, a mean placental perfusion rate of 176 ml/100 mg/min [20] was measured. Francis et al., applied FAIR ASL to compare the pattern of perfusion in normal versus IUGR-compromised pregnancies. Using perfusion maps that allow visual and statistical comparison of the fraction of perfusion, it was shown that the proportion of placentas with low perfusion rates was higher in the IUGR group than in the normal group (Fig. 2B) [21]. Reduced placental perfusion was also reported during the second trimester of pregnancy in the basal plate area in pregnancies complicated by small-for-gestational-age (SGA) fetuses. The findings were strongly associated with the perfusion values measured by diffusion MRI, and with impedance to flow in the uterine arteries, measured by Doppler ultrasound [22]. Duncan et al., found no differences in placental perfusion between normal and compromised pregnancies, although this study used a small sample size and low-field (0.5 T) MRI scanner, producing images with lower signal to noise [23].

## 4. Oxygenation studies

Due to the paramagnetic properties of deoxyhemoglobin, the oxygen state of the blood provides an endogenous MRI contrast mechanism. Compartmentalization of deoxygenated hemoglobin molecules creates magnetic susceptibility differences between red blood cells and blood plasma, which increases  $R_2^*$  relaxation rates. During a respiration challenge, changes in  $T_2^*$ -weighted BOLD signal intensity are affected mainly by changes in the saturation of

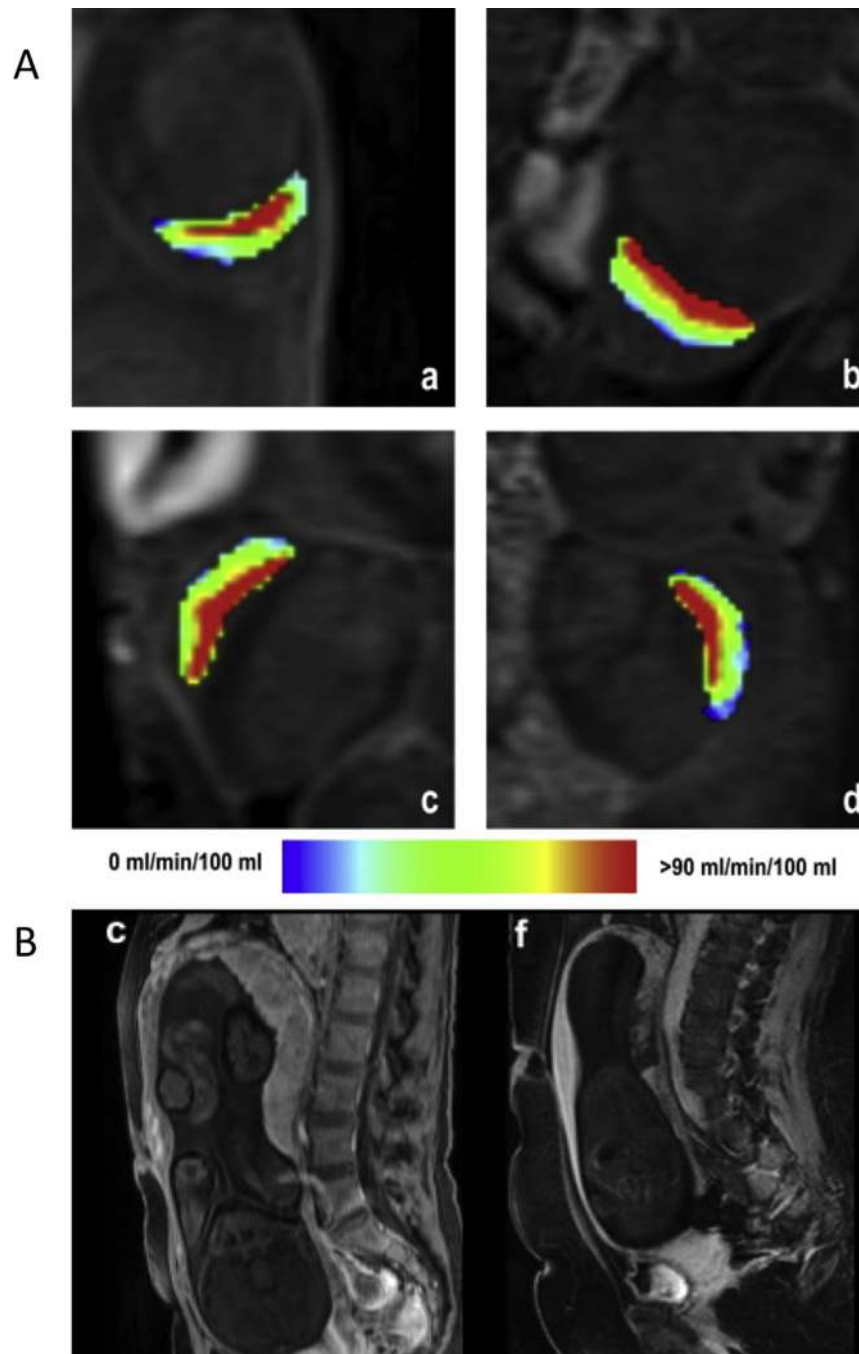


**Fig. 1.** Perfusion measurements using contrast agents. (A) Mouse placental perfusion maps calculated by the steepest slope model on embryonic day (E) 14.5 (a,b) and E16.5 (c,d), demonstrate, in all placentas, a high-flow compartment (red colored), which lies within the central labyrinth zone, and a low-flow compartment, which matches the peripheral labyrinth and the junctional zone. Reprinted from Ref. [6], with permission from Elsevier. (B) Human placental circulation in normal and IUGR pregnancies. 3D Contrast-enhanced, T<sub>1</sub>-weighted images acquired 2 min following administration of gadoterate meglumine in normal (c) and IUGR placentas (f). Normal placentas show a homogeneous signal increase, while IUGR-complicated placentas display many patchy, non-perfused areas. Reprinted from Ref. [17], with permission from Elsevier.

hemoglobin (i.e.,  $SO_2$ ), and, accordingly, can be used to image changes in tissue oxygenation.

BOLD MRI has been applied in animal models under different maternal respiration challenges, with changes in the fetoplacental BOLD signal intensity measured in response to the challenge. A hypercapnic respiration challenge in a maternal model of chronic fetal asphyxia resulted in a marked, generalized attenuation of the response in the placenta and fetal liver [24]. Recently, BOLD MRI was utilized in a rat uterine artery ligation model for IUGR during

maternal hyperoxygenation, demonstrating reduced response of compromised placentas compared with controls (Fig. 3A), and suggesting that this tool may be used to depict abnormalities in oxygenation related to impaired placental perfusion and IUGR [25,26]. Studies in sheep fetuses have shown that changes in cotyledon and fetal BOLD MRI signals are closely related to changes in fetal oxygenation estimated by fetal arterial hemoglobin saturation [27], and by fluorescent oxygen sensors inserted into the fetal liver [28].

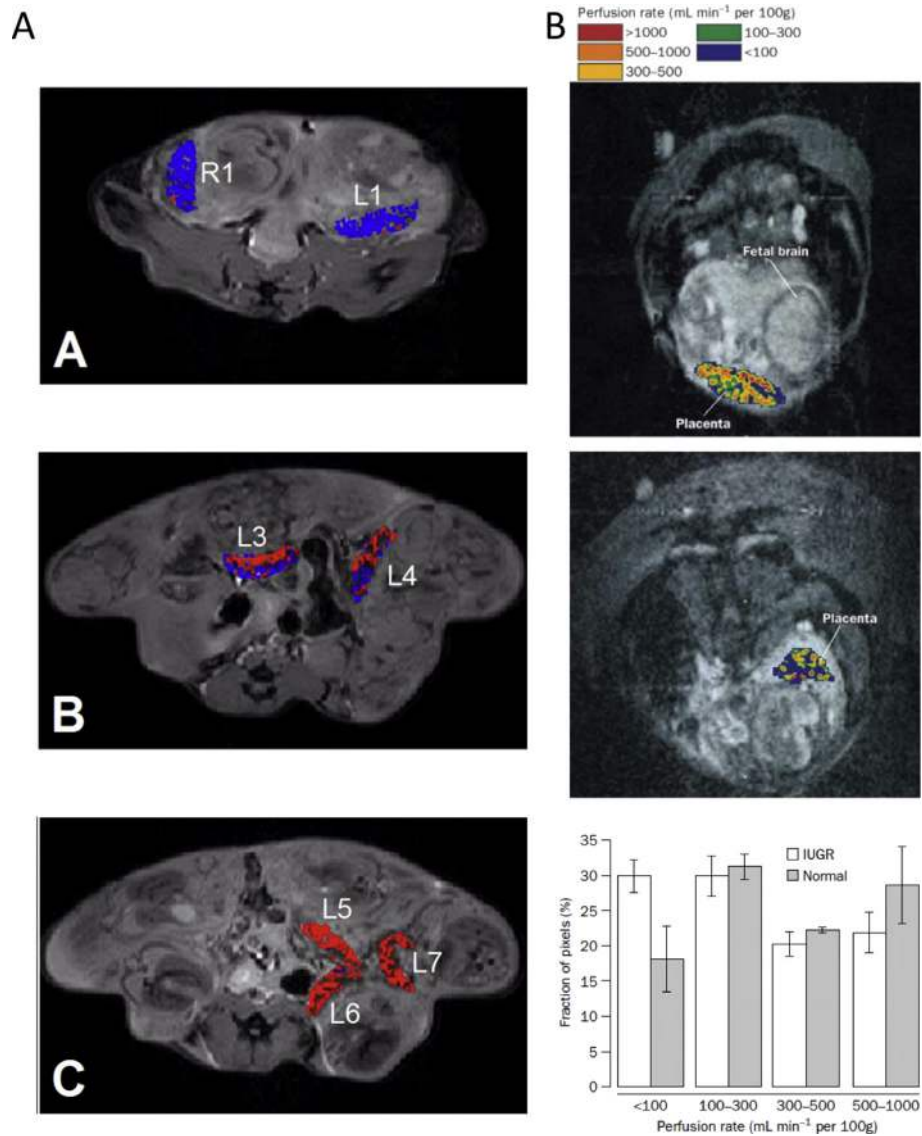


**Fig. 2.** Perfusion and flow measurements using endogenous MRI contrast. (A) Assessment of the arterial blood supply to mouse placenta of an ICR pregnant mouse (E17.5) via bidirectional arterial spin labeling (BD-ASL) MRI. A–C: Color-coded BD-ASL maps (red and blue, positive and negative BD-ASL values, respectively) show that placentas near the cervix (Panel A: L1, R1) have negative BD-ASL values, whereas those near the ovary (Panel C: L5–7) have positive values. Placentas located in the middle of the uterine horn (Panel B, L3–4) have a dispersive pattern of positive and negative BD-ASL values, suggesting a dual blood supply with separate arterial inputs from each of the feeding arteries [19]. (B) Left panel: Placental perfusion maps overlaid on an MRI image for: (top) a normal pregnancy and (bottom) a pregnancy complicated by IUGR. The placental perfusion rate in pregnancy complicated by IUGR is reduced, with many areas displaying infarction. Right panel: Histograms of placental perfusion fraction show a significant difference between IUGR and normal pregnancies in the distribution of perfusion categories. Reprinted from Ref. [21], with permission from Elsevier.

Real-time changes in BOLD MRI signals in response to changing oxygen levels have been demonstrated in human placenta and in a number of fetal organs during maternal oxygen challenge. Maternal hyperoxia was shown to increase placental oxygenation in healthy pregnancies, as measured by an increase in BOLD signal intensities (Fig. 3B) [29,30].

Oxygen-Enhanced (OE) MRI, which measures changes in  $T_1$  during a respiration challenge, is affected mainly by molecular oxygen, which shortens tissue  $T_1$  via dipolar interactions. Therefore, oxygen-induced changes in  $T_1$  reflect mainly the amount of dissolved oxygen in plasma and tissue fluid (i.e.,  $PO_2$ ), the partial pressure of oxygen. In combination with BOLD MRI, OE MRI was applied to investigate the placental oxygen environment over a range of gestations [31].

These preliminary clinical studies suggest that non-invasive MRI techniques are capable of measuring changes in placental and fetal

oxygenation under maternal respiration challenge, providing new possibilities for observing placental and fetal oxygenation status.

## 5. Microstructure

Diffusion weighted (DW) MRI is a sensitive approach for mapping the incoherent motions of water molecules, thereby providing insight into tissue microstructure at the micrometer level. DWI experiments typically report measurement of so-called apparent diffusion coefficients (ADCs).

Placental circulation can be roughly described as being composed of a maternal vascular system lined with trophoblast cells and a fetal system involving small blood capillaries. DW MRI studies are unable to resolve these structures due to the small sizes of cells and blood vessels. Moreover, placental mean ADC values may reflect various types of movements beyond free water

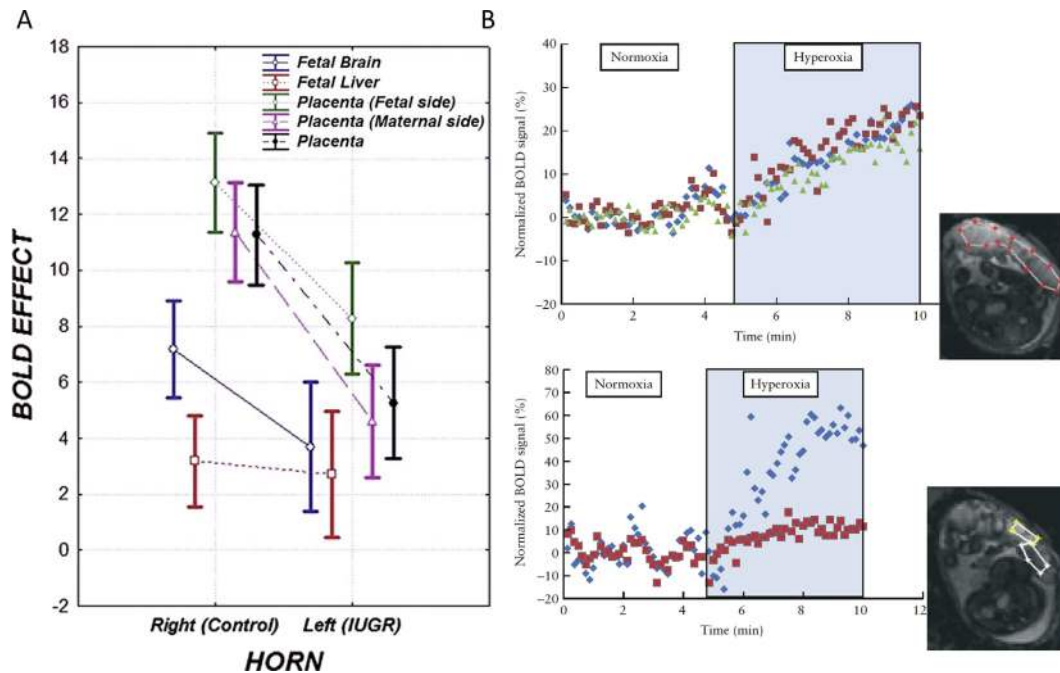


**Fig. 3.** Oxygenation studies: (A) Effect of maternal hyperoxygenation on the placenta and different fetal organs in a rat ligation model of IUGR. Box-and-whisker plots summarize changes in  $T_2^*$  values between hyperoxygenation and ambient air in placentas, fetal livers and fetal brains, in the normal and ligated IUGR uterine horns. There is a significant effect of maternal hyperoxygenation on BOLD SI in all organs. IUGR placentas show a significant reduction in the BOLD response to hyperoxygenation. Reprinted from Ref. [26], with permission from RSNA®; (B) Changes in human placental oxygenation BOLD signals during a maternal hyperoxic respiration challenge. Upper panel: Normalized BOLD SI of the entire placenta, in three different slices, shows a significant increase during maternal hyperoxia. Lower panel: Maternal and fetal areas within the placenta display different dynamics in response to maternal changes in oxygenation. Placental region of interests (ROIs) are shown in the inset images. Reprinted from Ref. [30], with permission from John Wiley and Sons.

diffusivity, including blood microcapillary flow, morphological restrictions acting on the molecular diffusion, and exchange, and it is impossible to distinguish between these motions using conventional DW MRI experiments. We therefore recently combined DW MRI with the emerging spatiotemporal encoding (SPEN) acquisition strategy, using a contrast-enhanced approach. By executing ADC measurements in the presence and absence of albumin-based contrast agent, b-BSAGdDTPA, and performing multi-exponential analysis of placental signal intensity, we were able to resolve multiple placental compartments and to characterize the movement of water in each compartment based on derived ADC values. Using this hybrid imaging strategy, we found that water motion in the maternal compartment is driven mainly by free diffusion, whereas water movement in the fetal compartment, which exhibited two orders of magnitude higher ADC values than the maternal ones, is dominated by flow. Finally, the movement of water in the trophoblast compartment, which displayed intermediate ADC values that were considerably higher than those expected for free diffusion, is dominated by contributions from fluid being actively filtered across the fetal–maternal barrier, and not by stationary intracellular water (Fig. 4A) [32].

Intravoxel incoherent motion (IVIM) is a derivative of DW MRI that attempts to distinguish between diffusion and perfusion of fluids. IVIM is appropriate for highly vascularized organs containing high blood fraction and a large, anisotropic perfusion component, like the placenta, and has been implemented in a rat uterine artery ligation model for IUGR to assess placental perfusion. Using this approach, it was possible to detect a reduced perfusion fraction in compromised placentas, relative to normal ones [33].

DW MRI has been widely applied over the last few years to assess human placental structures under normal conditions [34,35], and in high-risk pregnancies [22,36–42]. Using the IVIM

method, Moore, et al., identified differences between placentas of IUGR-complicated pregnancies and normal pregnancies. In normal pregnancies, different zones of blood movement were visible within the placentas, whereas in IUGR-complicated pregnancies, the placentas appeared far more homogenous, with their outer zones containing a significantly reduced proportion of moving blood compared to the normal cases (Fig. 4B) [36,37]. Other DW MRI studies in placentas complicated by IUGR have shown an overall reduction in placental diffusion [38], perfusion [22,39], and functional placental blood volume [39]. IVIM was also implemented in pregnancies complicated by PE, detecting a reduced fraction of mobile blood in the basal plate area of the placentas [40]. Sohlberg et al., found a clear difference between early onset (<34 weeks) and late onset (>34 week) PE, demonstrating a smaller perfusion fraction in early onset, but large perfusion in late onset, compared with normal [41]. Lastly, DW MRI has been shown to detect and define placental invasion in pregnancies complicated by placenta increta [42].

## 6. Metabolism

Magnetic Resonance Spectroscopy (MRS/NMR Spectroscopy) is a non-invasive method for determining the chemical structure of molecules, providing information about specific metabolites contained within selected regions of interest, which can be translated for assessment of the metabolic profile of tissues *in vivo*. NMR spectra can be used to detect specific metabolites; the area under each spectral peak is proportional to the concentration of the metabolite. The most common nuclei studied by MRS are hydrogen ( $^1\text{H}$ ) and phosphorus ( $^{31}\text{P}$ ).

As a result of numerous limitations imposed by the *in vivo* setting, most placental studies have utilized MRS techniques *in vitro*

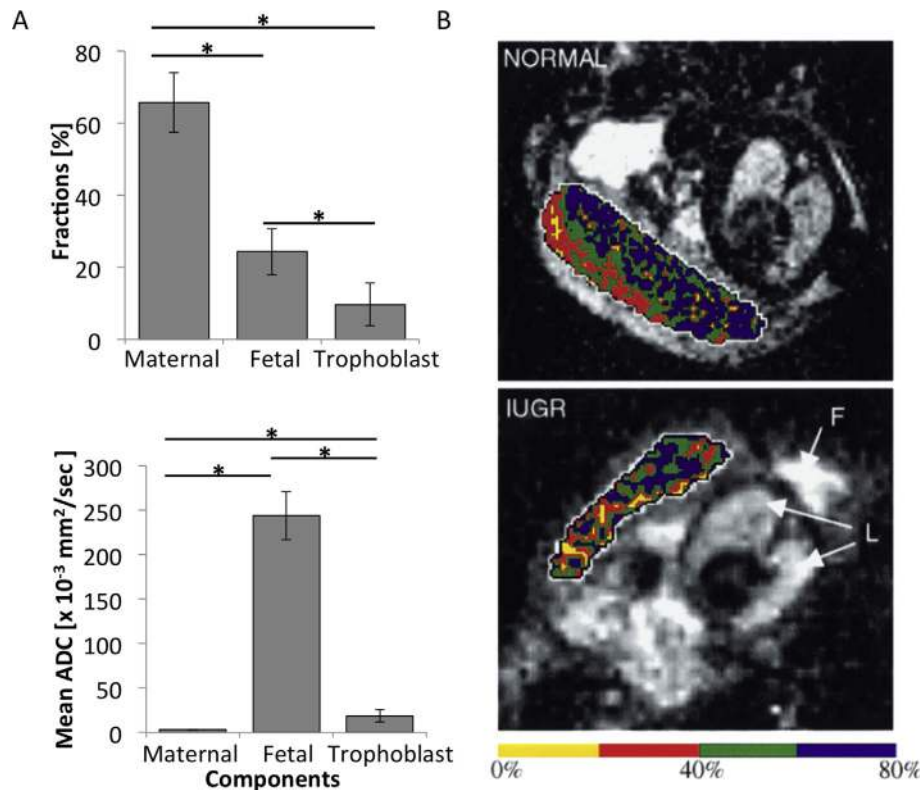


**Fig. 4.** Microstructure: (A) Resolving mouse placental structures using a hybrid strategy, combining DW MRI, contrast-enhanced under SPEN acquisition. Upper panel: Estimated placental compartmental fraction. Lower panel: Corresponding ADC values in each compartment. According to this analysis, maternal, fetal, and trophoblastic contributions constitute 66%, 24%, and 10% of overall placental volume, respectively. ADC values reveal a freely diffusive maternal blood pool, a strongly perfused fetal blood flow, and intermediate behavior for the trophoblastic labyrinth cell layer [32]. (B) Human placental perfusion fraction maps in normal and IUGR pregnancies, measured using IVIM. Perfusion fraction maps overlaid on MRI images for normal pregnancy (upper panel), indicating two zones of blood movement, and for pregnancy complicated by IUGR (lower panel), in which the placenta appears far more homogenous, with its outer zone containing a significantly reduced proportion of mobile blood. Reprinted from Ref. [37], with permission from Elsevier.

or *ex vivo* on fresh or frozen tissue samples. Due to the small sizes of placentas and the corresponding low sensitivities for detection of metabolites, no studies have been performed in animal models. Clinical studies are currently restricted due to the sensitivity of the imaging coil, and thus are limited to women with anterior placentas and low body fat.

Phospholipid metabolism has been studied in normal human placenta by *in vivo*  $^{31}\text{P}$  MRS [43]. Recently, placental membrane metabolism has been investigated using  $^{31}\text{P}$  MRS in women with normal pregnancies and those with early (<34 weeks) and late (>34 weeks) onset PE. Phosphodiester (PDE) spectral intensity and the PDE-to-phosphomonoester spectral intensity ratio (PDE/PME) are factors associated with cell-membrane degradation and formation. It was shown that both PDE intensity and the PDE/PME ratio increased with increasing gestational age in normal pregnancy, and these increases were larger in early onset PE than in late normal pregnancy (Fig. 5A). These results indicate that with increasing gestational age in normal pregnancy, and in early onset PE, increased cell degradation and increased apoptosis may occur [44].

$^1\text{H}$  MRS has been utilized to assess the metabolic profile of placental tissue in healthy and IUGR pregnancies. In healthy pregnancies, a significant choline (Cho)/lipid ratio was detected, whereas in IUGR-complicated pregnancies, Cho peak was severely attenuated or absent from all placentas, indicative of a reduction in cell turnover (Fig. 5B) [45]. A proof-of-concept study was performed assessing placental glutamine and glutamate (Glx) to Cho ratios (Glx/Cho) in healthy and IUGR pregnancies. The Glx/Cho ratio

was lower for IUGR placentas than in those of matched controls [46]. These studies suggest that abnormal placental  $^1\text{H}$  MR spectra can serve as an early biomarker of altered placental metabolism. *In vivo* MRS techniques could be greatly improved with the use of improved coil design to provide a more homogeneous transmitting field, which would provide better localization and allow comparison of slices recorded at different depths.

## 7. Summary and future perspectives

Early identification of high risk fetuses and timing of delivery are among the main challenges in modern day obstetrics. Functional MRI of the placenta can provide valuable information on several important physiological parameters, including blood flow, perfusion and oxygenation status, which could potentially serve as sensitive biomarkers for negative changes, even at early pregnancy stages. However, despite the availability of numerous MRI techniques for studying placental function, *in vivo* studies of the placenta are limited, and, currently, there is no accepted MRI-based definition of normal or pathological placental function. This may be due, in part, to several technical challenges, including the lack of consensus on imaging protocols, poor image quality, especially in low field magnets, and the limited availability of MRI scanners, relative to US, preventing the acquisition of data from a large number of pregnancies. Additional obstacles arise from the complex vascular architecture of the placenta, which often leads to inconclusive data and inadequate theories for describing the signal

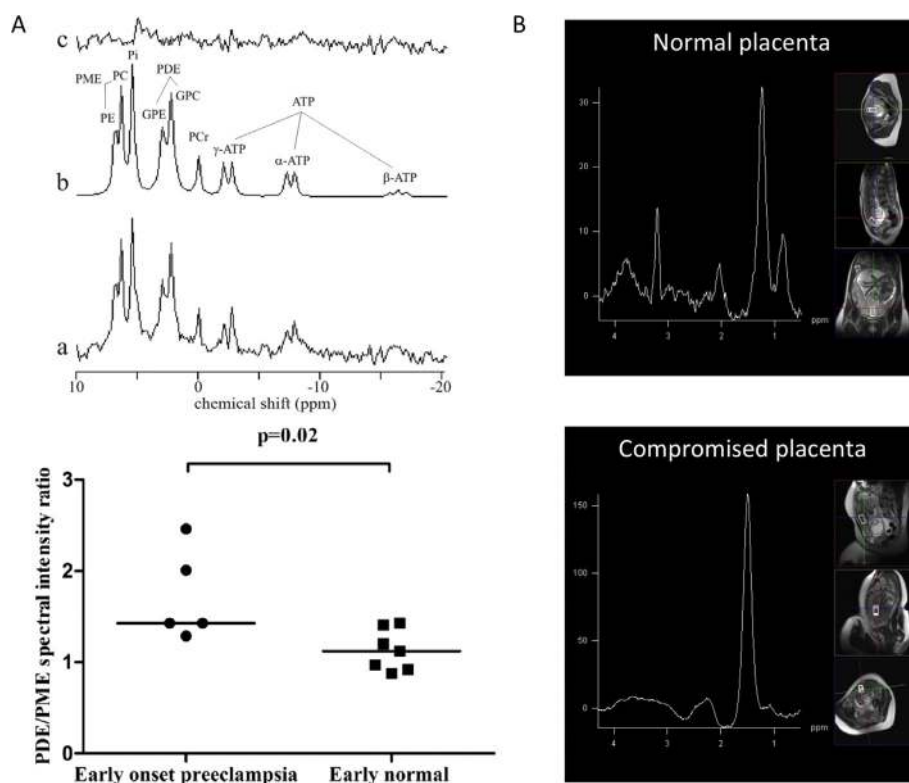


**Fig. 5.** Metabolism: (A) <sup>31</sup>P MRS in healthy and IUGR complicated pregnancies: Upper panel: representative <sup>31</sup>P spectrum of a normal human placenta at 38 weeks gestation (a), fitted spectrum (b), and residual (c). Spectral intensities of the following metabolites were evaluated: phosphomonoesters (PME = phosphoethanolamine (PE) + phosphocholine (PC)); inorganic phosphate; phosphodiester (PDE = glycerophosphoethanolamine (GPE) + glycerophosphocholine (GPC)); phosphocreatine (PCr); and adenosine triphosphate (ATP). Lower panel: Scatter plot displaying PDE/PME spectral intensity ratio in early onset (<34 weeks) PE versus normal pregnancy. Women with early onset preeclampsia have a higher PDE/PME spectral intensity ratio than women with normal pregnancies. Reprinted from Ref. [44], with permission from Elsevier. (B) <sup>1</sup>H MRS: upper panel: placental <sup>1</sup>H MRS spectrum acquired from normal human pregnancy. Choline and lipid spectral peaks appear at frequencies of 3.21, 1.3 and 0.9 parts per million (ppm), respectively. Lower panel: Placental <sup>1</sup>H MRS spectrum acquired from IUGR-compromised pregnancy. The lipid spectral peak appears at a frequency of 1.42 ppm. The choline peak is below the level of reliable detection. Reprinted from Ref. [45], with permission from PLOS ONE.

behavior, and, finally, to a missing link between the MRI-derived parameters and physiological factors.

To advance the field, there is a need for more basic research studies using animal models to enhance the understanding of pregnancy complications and to expand the development of novel imaging tools for studying placental function. As interpretation of MRI data can be very complex and is often ambiguous, there is a need for more robust computational methods and for the standardization of information that can provide absolute quantification of placental functional metrics, independent of magnetic-field strength, image-sequence parameters, and scientific center. Separating and distinguishing different placental compartments could prevent bias from averaging their different contributions. Moreover, the use of hybrid methods, combining several MRI techniques, may provide new information, allow comparison between different parameters, and reduce the costs and number of patients/animals. Finally, switching to higher field strengths may offer some advantages, including improved sensitivity and image quality, longer T<sub>1</sub> relaxation time constants, which increases the time window accessible for transfer of label before recovery of the signal, and higher T<sub>2</sub><sup>\*</sup>-based contrast, as T<sub>2</sub><sup>\*</sup> effects are more pronounced in higher field strengths. However, artifacts worsen with increasing magnetic strengths, and the specific absorption rates (SAR) are increased, adding safety concerns. In clinical settings, magnetic-field strength of 3T may provide a good compromise between all of these factors, whereas in small-animal models, higher field

strength, such as 9.4T, should be used to enable high quality images despite the small sizes of placental structures.

We hope that in the near future, many of these techniques will be available for routine clinical practice to distinguish between normal and compromised pregnancies. Methods that offer information that is not available using US assessments, such as fetoplacental oxygenation status, or other methods that do not require the use of exogenous contrast agents, would be of particular value.

#### Conflict of interest

The authors have no conflict of interest to declare.

#### Acknowledgments

This work was supported by the 7th Framework European Research Council Advanced grant 232640-IMAGO (to MN), and by the United States – Israel Binational Science Foundation grant 2011405 (BSF to MN and JRG). M.N. is the incumbent of the Helen and Morris Mauerberger Chair in Biological Sciences.

#### Appendix A. Supplementary data

Supplementary data related to this article can be found at <http://dx.doi.org/10.1016/j.placenta.2015.04.003>.

## References

- [1] Salomon LJ, Siauve N, Balvay D, Cuenod CA, Vayssettes C, Luciani A, et al. Placental perfusion MR imaging with contrast agents in a mouse model. *Radiology* 2005;235(1):73–80.
- [2] Taillieu F, Salomon LJ, Siauve N, Clement O, Faye N, Balvay D, et al. Placental perfusion and permeability: simultaneous assessment with dual-echo contrast-enhanced MR imaging in mice. *Radiology* 2006;241(3):737–45.
- [3] Salomon LJ, Siauve N, Taillieu F, Balvay D, Vayssettes C, Frija G, et al. In vivo dynamic MRI measurement of the noradrenaline-induced reduction in placental blood flow in mice. *Placenta* 2006;27(9–10):1007–13.
- [4] Alison M, Quibel T, Balvay D, Autret G, Bourillon C, Chalouhi GE, et al. Measurement of placental perfusion by dynamic contrast-enhanced MRI at 4.7 T. *Invest Radiol* 2013;48(7):535–42.
- [5] Tomlinson TM, Garbow JR, Anderson JR, Engelbach JA, Nelson DM, Sadovsky Y. Magnetic resonance imaging of hypoxic injury to the murine placenta. *Am J Physiol Regul Integr Comp Physiol* 2010;298(2):R312–9.
- [6] Remus CC, Sedlacik J, Wedegaertner U, Arck P, Hecher K, Adam G, et al. Application of the steepest slope model reveals different perfusion territories within the mouse placenta. *Placenta* 2013;34(10):899–906.
- [7] Kording F, Forkert ND, Sedlacik J, Adam G, Hecher K, Arck P, et al. Automatic differentiation of placental perfusion compartments by time-to-peak analysis in mice. *Placenta* 2014.
- [8] Deloison B, Siauve N, Aimot S, Balvay D, Thiam R, Cuenod CA, et al. SPIO-enhanced magnetic resonance imaging study of placental perfusion in a rat model of intrauterine growth restriction. *BJOG* 2012;119(5):626–33.
- [9] Plaks V, Sapoznik S, Berkovitz E, Haffner-Krausz R, Dekel N, Harmelin A, et al. Functional phenotyping of the maternal albumin turnover in the mouse placenta by dynamic contrast-enhanced MRI. *Mol Imaging Biol* 2011;13(3):481–92.
- [10] Plaks V, Berkovitz E, Vandoorne K, Berkutzki T, Damari GM, Haffner R, et al. Survival and size are differentially regulated by placental and fetal PKBalpha/AKT1 in mice. *Biol Reprod* 2011;84(3):537–45.
- [11] Kay HH, Knop RC, Mattison DR. Magnetic resonance imaging of monkey placenta with manganese enhancement. *Am J Obstet Gynecol* 1987;157(1):185–9.
- [12] Panigel M, Wolf G, Zeleznick A. Magnetic resonance imaging of the placenta in rhesus monkeys, *Macaca mulatta*. *J Med Primatol* 1988;17(1):3–18.
- [13] Frias AE, Schabel MC, Roberts VH, Tudorica A, Grigsby PL, Oh KY, et al. Using dynamic contrast-enhanced MRI to quantitatively characterize maternal vascular organization in the primate placenta. *Magn Reson Med Off J Soc Magn Reson Med* 2014;152.
- [14] Barkhof F, Heijboer RJ, Algra PR. Inadvertent i.v. administration of gadopentetate dimeglumine during early pregnancy. *AJR Am J Roentgenol* 1992;158(5):1171.
- [15] Marcos HB, Semelka RC, Worawattanakul S. Normal placenta: gadolinium-enhanced dynamic MR imaging. *Radiology* 1997;205(2):493–6.
- [16] Palacios Jaraquemada JM, Bruno C. Gadolinium-enhanced MR imaging in the differential diagnosis of placenta accreta and placenta percreta. *Radiology* 2000;216(2):610–1.
- [17] Brunelli R, Masselli G, Parasassi T, De Spirito M, Papi M, Perrone G, et al. Intervillous circulation in intra-uterine growth restriction. Correlation to fetal well being. *Placenta* 2010;31(12):1051–6.
- [18] Avni R, Raz T, Biton IE, Kalchenko V, Garbow JR, Neeman M. Unique in utero identification of fetuses in multifetal mouse pregnancies by placental bidirectional arterial spin labeling MRI. *Magn Reson Med* 2012;68(2):560–70.
- [19] Raz T, Avni R, Addadi Y, Cohen Y, Jaffa AJ, Hemmings B, et al. The hemodynamic basis for positional- and inter-fetal dependent effects in dual arterial supply of mouse pregnancies. *PLoS One* 2012;7(12):e52273.
- [20] Gowland PA, Francis ST, Duncan KR, Freeman AJ, Issa B, Moore RJ, et al. In vivo perfusion measurements in the human placenta using echo planar imaging at 0.5 T. *Magn Reson Med* 1998;40(3):467–73.
- [21] Francis ST, Duncan KR, Moore RJ, Baker PN, Johnson IR, Gowland PA. Non-invasive mapping of placental perfusion. *Lancet* 1998;351(9113):1397–9.
- [22] Derwig I, Lythgoe DJ, Barker GJ, Poon L, Gowland P, Yeung R, et al. Association of placental perfusion, as assessed by magnetic resonance imaging and uterine artery Doppler ultrasound, and its relationship to pregnancy outcome. *Placenta* 2013;34(10):885–91.
- [23] Duncan KR, Gowland P, Francis S, Moore R, Baker PN, Johnson IR. The investigation of placental relaxation and estimation of placental perfusion using echo-planar magnetic resonance imaging. *Placenta* 1998;19(7):539–43.
- [24] Abramovitch R, Corchia N, Elchala U, Ginosar Y. Changes in placental and fetal organ perfusion during chronic maternal hypoxia: assessment by BOLD MRI during brief hypercapnic and hyperoxic challenge. *Proc Int Soc Mag Reson Med* 2011;19.
- [25] Aimot-Macron S, Salomon LJ, Deloison B, Thiam R, Cuenod CA, Clement O, et al. In vivo MRI assessment of placental and foetal oxygenation changes in a rat model of growth restriction using blood oxygen level-dependent (BOLD) magnetic resonance imaging. *Eur Radiol* 2013;23(5):1335–42.
- [26] Chalouhi GE, Alison M, Deloison B, Thiam R, Autret G, Balvay D, et al. Feto-placental oxygenation in an intrauterine growth restriction rat model by using blood oxygen level-dependent MR imaging at 4.7 T. *Radiology* 2013;269(1):122–9.
- [27] Wedegaertner U, Tchirikov M, Schafer S, Priest AN, Kooijman H, Adam G, et al. Functional MR imaging: comparison of BOLD signal intensity changes in fetal organs with fetal and maternal oxyhemoglobin saturation during hypoxia in sheep. *Radiology* 2006;238(3):872–80.
- [28] Sorensen A, Pedersen M, Tietze A, Ottosen L, Duus L, Ulldbjerg N. BOLD MRI in sheep fetuses: a non-invasive method for measuring changes in tissue oxygenation. *Ultrasound Obstet Gynecol* 2009;34(6):687–92.
- [29] Sorensen A, Peters D, Simonsen C, Pedersen M, Stausbol-Gron B, Christiansen OB, et al. Changes in human fetal oxygenation during maternal hyperoxia as estimated by BOLD MRI. *Prenat Diagn* 2013;33(2):141–5.
- [30] Sorensen A, Peters D, Frund E, Lingman G, Christiansen O, Ulldbjerg N. Changes in human placental oxygenation during maternal hyperoxia estimated by blood oxygen level-dependent magnetic resonance imaging (BOLD MRI). *Ultrasound Obstet Gynecol* 2013;42(3):310–4.
- [31] Huen I, Morris DM, Wright C, Parker GJ, Sibley CP, Johnstone ED, et al. R1 and R2 \* changes in the human placenta in response to maternal oxygen challenge. *Magn Reson Med* 2013;70(5):1427–33.
- [32] Solomon E, Avni R, Hadas R, Raz T, Garbow JR, Bendel P, et al. Major mouse placental compartments revealed by diffusion-weighted MRI, contrast-enhanced MRI, and fluorescence imaging. *Proc Natl Acad Sci U S A* 2014;111(28):10353–8.
- [33] Alison M, Chalouhi GE, Autret G, Balvay D, Thiam R, Salomon LJ, et al. Use of intravoxel incoherent motion MR imaging to assess placental perfusion in a murine model of placental insufficiency. *Investig Radiol* 2013;48(1):17–23.
- [34] Manganaro L, Fierro F, Tomei A, La Barbera L, Savelli S, Sollazzo P, et al. MRI and DWI: feasibility of DWI and ADC maps in the evaluation of placental changes during gestation. *Prenat Diagn* 2010;30(12–13):1178–84.
- [35] Sivrioglu AK, Ozcan U, Turk A, Ulus S, Yildiz ME, Sonmez G, et al. Evaluation of the placenta with relative apparent diffusion coefficient and T2 signal intensity analysis. *Diagn Intervent Radiol* 2013;19(6):495–500.
- [36] Moore RJ, Issa B, Tokarczuk P, Duncan KR, Boulby P, Baker PN, et al. In vivo intravoxel incoherent motion measurements in the human placenta using echo-planar imaging at 0.5 T. *Magn Reson Med* 2000;43(2):295–302.
- [37] Moore RJ, Strachan BK, Tyler DJ, Duncan KR, Baker PN, Worthington BS, et al. In utero perfusing fraction maps in normal and growth restricted pregnancy measured using IVIM echo-planar MRI. *Placenta* 2000;21(7):726–32.
- [38] Bonel HM, Stolz B, Diedrichsen L, Frei K, Saar B, Tutschek B, et al. Diffusion-weighted MR imaging of the placenta in fetuses with placental insufficiency. *Radiology* 2010;257(3):810–9.
- [39] Javor D, Nasel C, Schweim T, Dekan S, Chalubinski K, Prayer D. In vivo assessment of putative functional placental tissue volume in placental intra-uterine growth restriction (IUGR) in human fetuses using diffusion tensor magnetic resonance imaging. *Placenta* 2013;34(8):676–80.
- [40] Moore RJ, Ong SS, Tyler DJ, Duckett R, Baker PN, Dunn WR, et al. Spiral artery blood volume in normal pregnancies and those compromised by preeclampsia. *NMR Biomed* 2008;21(4):376–80.
- [41] Sohlberg S, Mulic-Lutvica A, Lindgren P, Ortiz-Nieto F, Wikstrom AK, Wikstrom J. Placental perfusion in normal pregnancy and early and late preeclampsia: a magnetic resonance imaging study. *Placenta* 2014;35(3):202–6.
- [42] Morita S, Ueno E, Fujimura M, Muraoka M, Takagi K, Fujibayashi M. Feasibility of diffusion-weighted MRI for defining placental invasion. *J Magn Reson Imaging* 2009;30(3):666–71.
- [43] Weindling AM, Griffiths RD, Garden AS, Martin PA, Edwards RH. Phosphorus metabolites in the human placenta estimated in vivo by magnetic resonance spectroscopy. *Arch Dis Child* 1991;66(7 Spec No):780–2.
- [44] Sohlberg S, Wikstrom AK, Olovsson M, Lindgren P, Axelsson O, Mulic-Lutvica A, et al. In vivo (3)1P-MR spectroscopy in normal pregnancy, early and late preeclampsia: a study of placental metabolism. *Placenta* 2014;35(5):318–23.
- [45] Denison FC, Semple SI, Stock SJ, Walker J, Marshall I, Norman JE. Novel use of proton magnetic resonance spectroscopy (1HMRS) to non-invasively assess placental metabolism. *PLoS One* 2012;7(8):e42926.
- [46] MacMaught G, Semple S, Gray C, Simpson M, Norman J, Walker J, et al. Reduced glutamate: choline ratio by 1H MRS as a biomarker for placental insufficiency in the growth restricted fetus. *Arch Dis Child Fetal Neonatal Ed* 2014;99(Suppl. 1):A85.